MAPPING NMR T_2 TO CAPILLARY PRESSURE

Andrea Valori, Farhan Ali, Ahmad Al-Zoukani, Reza Taherian
Schlumberger Dhahran Carbonate Research, Saudi Arabia

This paper was prepared for presentation at the International Symposium of the Society of Core Analysts held in Avignon, France, 8-11 September, 2014

ABSTRACT

Starting with a fully water saturated carbonate core plug we replaced the water content with air using small incremental capillary pressure steps.
At each capillary pressure we measured the T_2 distribution and calculated the differential T_2 distribution. This process allows determination of the T_2 components associated with the fraction of water that leaves the rock at each capillary pressure. The differential T_2 spectra were converted to pore size while the pressure data was converted to the throat size and their ratio was calculated at each pressure differential. The results show pore size to throat size ratios on the order of 0.25-2.25. The scatter in the results was attributed to similar size pores which are connected to different throat sizes and different size pores which are connected to similar throat sizes.

INTRODUCTION

Fluid flow in porous media is a crucial step in reservoir management. Furthermore, understanding the flow in the rock is at the core of reservoir simulation and production estimation.
NMR is sensitive to the pore size distribution of porous materials [1], [2], while the applied capillary pressure in a flooding experiment is related to the throat size by the Young-Laplace equation.
Attempts to relate NMR to MICP have not been very successful because they are related to two different structural properties of the porous medium [3]. The differences should not be surprising, since the two techniques measure different parameters. In this paper we attempt a novel approach to address pore size to throat size relationship.

NMR T_2 interpretation

NMR T_2 relaxation analysis can be used as a mean to get Pore Size Distribution (PSD) [1], [2]. This is because within the same pore there are two different relaxation regimes; a faster one affecting the molecules on the surface of the pore with characteristic time $T_{2,surface}$, and a much slower one, affecting the molecules in the bulk of the pore and occurring with characteristic time $T_{2,bulk}$. Because of a very fast exchange between the two types of molecules, the observed T_2 decay is proportional to the volume weighted average between the two populations. The volume of surface bound fluid is δS where S is

the pore surface areas and δ is the thickness of the fast relaxing layer. Similarly the volume of bulk fluid is, V-$\delta S \sim V$. Equation (1), below, demonstrates how the volume average of the active T_2's leads to a surface relaxivity term and the Surface to Volume ratio of the pore (S/V). In (1) the two parameters $T_{2,\text{surface}}$ and bound fluid thickness δ are in a single parameter $\rho = {\delta}/{T_{2,\text{surface}}}$ called relaxivity. Note that the dimension of ρ is a velocity.

$$\frac{1}{T_{2,obs}} = \frac{1}{T_{2,\text{bulk}}} + \rho\frac{S}{V} \quad (1)$$

Sample preparation

Starting from a fully water saturated carbonate outcrop cylindrical core plug (1.5"diameter, 2" long), we removed the water by centrifugation in air at small increasing centrifugal (capillary) pressure steps. At each step we acquired an NMR T_2 distribution of the core plug sample.

RESULTS AND DISCUSSION

The entire dataset obtained is presented in Figure 1 a), where all the T_2 distributions are presented in a surface plot. Each horizontal line represents a T_2 distribution for a different applied capillary pressure. The amplitude of the T_2 distributions is colour coded from red (high) to blue (low).

As the pressure increases, the stronger peak in Figure 1 a) located at $T_2 > 0.1$ s quickly decreases in amplitude and disappears almost completely at pressures of about 5 PSI. The starting T_2 distributions (high Sw's) are bimodal with a trough at 0.02 sec. We will use this number as a "visual" cut-off to separate bound and free fluid (the cut-off is shown as the green line in Figure 1 a). We also show the standard T_2 cut-off value for carbonates (0.1 s) in magenta. Figure 1 b) shows the differential T_2 distributions. These are obtained by subtracting the echo time decays acquired at two consecutive capillary pressures and Laplace inverting the subtracted (differential) time data. Here it is important to note that the subtraction is done in the time domain. Subtraction in the T_2 domain tends to be too unstable to give meaningful results. The differential T_2 peaks have smaller intensities and are internally re-normalised to obtain Figure 1 b and should not be compared with the intensities of Figure 1 a). Figure 1 c) shows the full T_2 distribution at Sw1 (100% water saturation) and a selection of three differential T_2 distributions. In this case the distributions have not been renormalized to allow comparison of amplitudes. We note that some of the differential T_2 distributions show a tail towards short T_2 values, although these tails are barely visible at the plotted scale. To highlight the presence of the tail, two of the differential T_2 distributions are also plotted with their amplitude multiplied by 5 (dashed lines). The tail at short T_2 values can be interpreted as the presence of pores of a wide range of body sizes but with similar pore throats and therefore draining at the same capillary pressure.

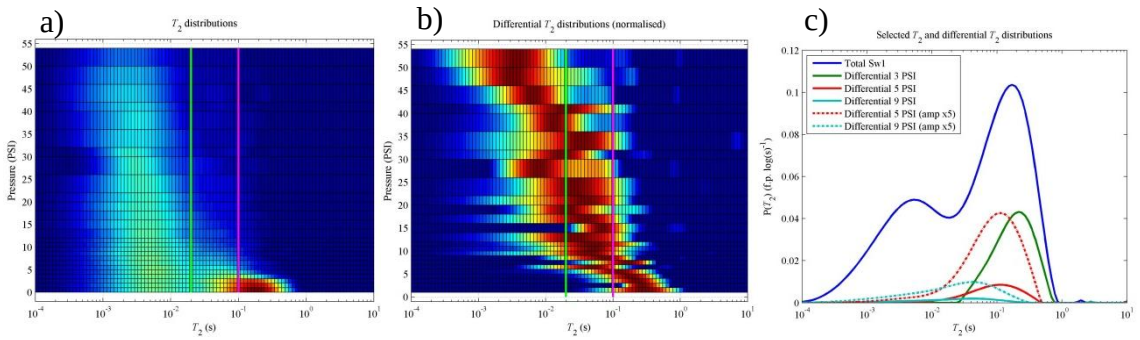

Figure 1: a) T_2 distributions as a function of applied capillary pressure. The vertical lines represent the standard cut-off for carbonate of 0.1 s (magenta) and the visual one of 0.02 s. b): differential T_2 distributions. These are the T_2 distributions of the removed fluid only. c) Sw=1 plot and comparison with a selection of differential T_2 distributions non-renormalized; therefore the amplitudes can be compared. The dashed lines have their amplitude multiplied by 5 to show the tail at short T_2 values.

Using the visual cut-off mentioned above we can compute the bound and free fluid volumes as it is typically done in standard NMR interpretation, but in our case we can do that as a function of applied capillary pressure. These results are plotted in Figure 2 (left). Also, the total NMR signal as a function of increasing capillary pressure is plotted in black. The total signal drops sharply at pressures between 0-5 PSI. This is consistent with the observations in Figure 1 a). We note an intermediate slope between about 5 and 10 PSI. This is followed by slow signal decay at higher pressures.

We note that for the fully water saturated and the first two pressures, the volume of free fluid is larger than the bound fluid, but above about 2.5 PSI the free fluid drops below the bound fluid. The Bound Fluid Volume (BFV) stays virtually constant up to about 8 PSI, then start decreasing very slowly. The Free Fluid Volume (FFV) instead decreases sharply for the early capillary pressure steps.

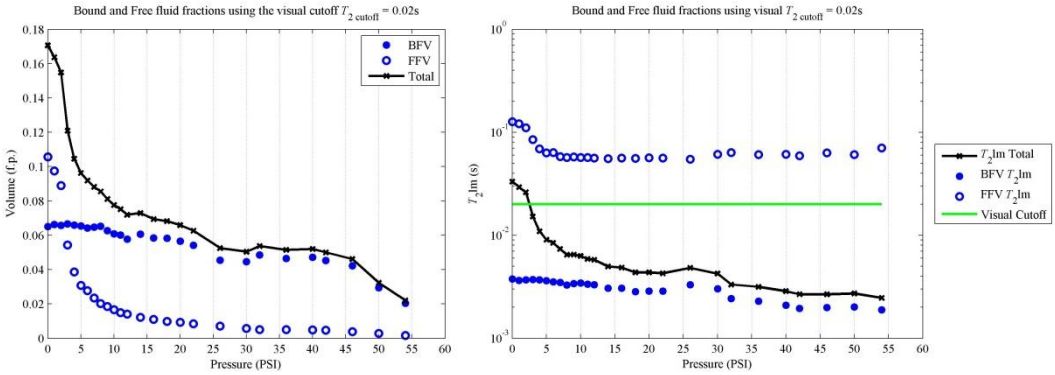

Figure 2 Left: free and bound fluid factions. Right: logarithmic average of the T_2 distribution for the Free and Bound fluid fractions

Once the signal in the T_2 domain is separated into bound and free fluid regions, we can calculate the logarithmic T_2 mean ($T_{2\mathrm{lm}}$) for the two fluid fractions. Figure 2 (right) shows the results of such calculations.

Estimation of bound and free water volumes can also be performed using the differential T_2 data. In this case there is no need to use a cut-off and either the peak (Figure 3, right) or the logarithmic mean (Figure 3, left) of the differential T_2 can be used. The

disadvantage of Figure 3 is that other lines of reasoning should be used to separate the bound and free water. For example, the data in Figure 3 (left) clearly shows a fast slope vs pressure at low pressures which may be attributed to the production of free water. Such assignment is consistent with the findings from Figure 2.

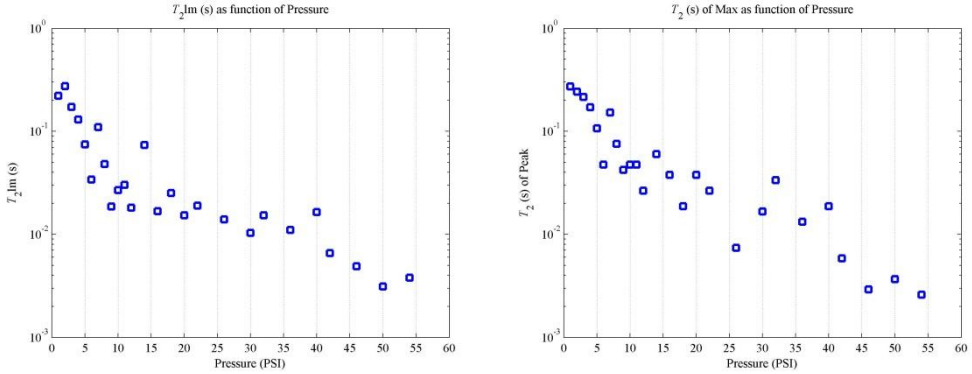

Figure 3 Left: T_2 logarithmic average of the differential T_2 distributions, as a function of applied capillary pressure. Right: T_2 value for the peak of the differential T_2 distributions

Using equation (1), we can assume a reasonable value for the relaxivity and use the well know value for $T_{2,bulk}$ to solve for S/V. Since these measurements involved water as the only source of NMR signal, the value of $T_{2,bulk}$ is well known and is 2.3 s. The exact value however, is not needed for the following analysis since for $T_{2,\,obs} << T_{2,\,bulk} \approx 2$ s small changes in $T_{2,bulk}$ do not cause any significant differences. This is the case for all the data presented here (see Figure 1 a) and c)). Indeed, after the first few pressure steps, the $1/T_{2,bulk}$ can be completely neglected. The choice of the relaxivity ρ, however, has a stronger impact on the S/V determination. Values in the literature vary widely, with a fairly common belief that sandstones have higher relaxivity than carbonate rocks. Typical values for carbonate range from 5 to 30 μm/s. For the following analysis we used $\rho = 20$ μm/s; other values will lead to an additional multiplicative factor. For this calculation we used the T_2 value of the maximum of the differential T_2 distributions; however, as shown in Figure 3 these do not differ significantly from the logarithmic mean T_2 values.

Since typically $T_{2,obs}$ is a wide distribution (see Figure 1 a)) especially at high saturations (low pressures) inverting equation (1) does not lead to a single value for S/V, but rather a distributions of ratios which are very difficult to interpret. To avoid this, we applied the procedure to the differential T_2 instead. In this case the approximation of a single T_2 value (and therefore single S/V ratio) is more acceptable. The results are reported in Figure 4. Under the assumption of a specific geometry, the S/V ratio can be further converted to a "characteristic pore size" R. For example, assuming cylindrical pores with radius r and length l:

$$\frac{S}{V} = \frac{2\pi r l}{\pi r^2 l} = \frac{2}{r} \qquad (2)$$

The scale on the right hand side of Figure 4 refers to the characteristic pore radius calculated using Equation (2).

The capillary pressure can be converted to pore throat size following the Young–Laplace Equation (3) where $\gamma = 72*10^{-3}$ N/m is the air/water interfacial tension and θ the contact angle (set equal to 0 in our case since the rock is water wet). The right panel of Figure 4 shows the same data as in the left panel, but the pore throat size calculated from Equation (3) is used for horizontal axis.

$$r = \frac{2\gamma\, cos\theta}{P_c} \tag{3}$$

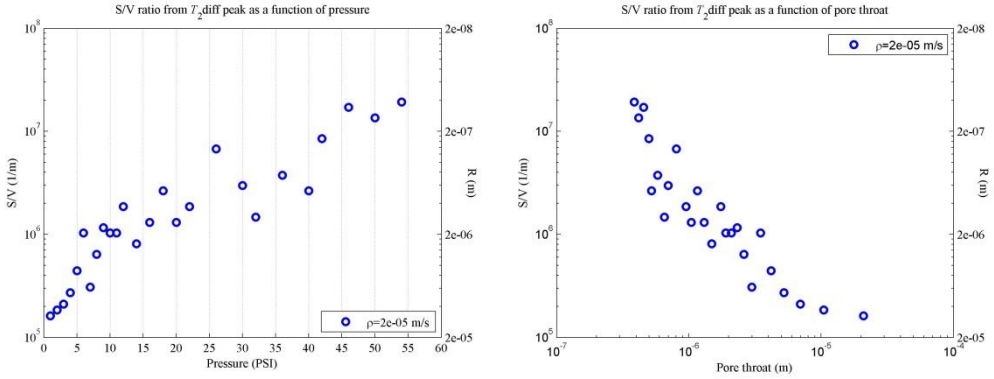

Figure 4 Left: Surface over Volume ratio calculated from Equation (1). The right hand side axis indicates the pore radius assuming cylindrical geometry. Right: the same data but plotted as a function of pore throat.

Re-arranging the data in Figure 4, we can extract another useful piece of information: the body to throat ratio of the pores emptied at each pressure step. This result is plotted in Figure 5.

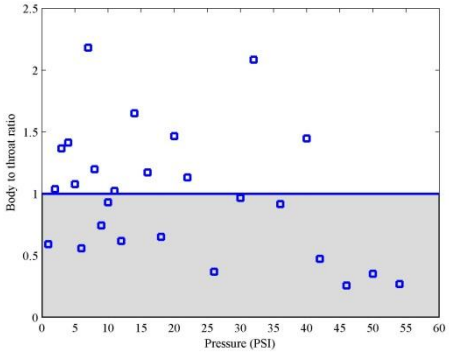

Figure 5 Body to throat ratio for the pores emptied at each pressure step. The shaded area is the region considered to be "unphysical"

Figure 5 shows some fluctuations in the plotted body to throat ratio for each pressure step; however, the ratio fluctuates is the range between about 0.25 and 2.25. Values below 1 are unphysical since for a single pore, the pore throat can't be larger than the pore body; however note that the measurement at each pressure is an average of a relatively narrow distribution of pores and throats. In addition we have used an arbitrary relaxivity value of $2\cdot10^{-5}$ m/s and a higher relaxivity value can shift the entire data points upward. A relaxivity higher than $7\cdot10^{-5}$ m/s brings all the points on the physical region of the plane. Furthermore, as Figure 6 (left) shows, the same size pores may be connected to

different size throats and thus will be emptied at different Pc's. Similarly as Figure 6 (right) shows, different pore sizes may be connected to the same throat size and empty at the same Pc. The results shown in Figure 5, therefore, have to be interpreted in an average fashion.

Figure 6 Left, two pores having the same size (and therefore T_2) but different throat (and therefore different entry pressures). Right, two pores of different size (and therefore T_2) but the same pore throat (and therefore same entry pressure)

CONCLUSIONS

- Subtracting two time domain NMR signals, obtained at two different capillary pressures, leads to differential echo time data which can be inverted to provide differential T_2 distributions.
- The differential T_2 distributions are narrower and are subsets of the entire T_2 distribution. Each subset originates from the pores that have been emptied as a result of applying the differential capillary pressure.
- The narrow differential T_2 can be used to calculate an average pore body to pore throat ratio. The ratio is approximately 0.25-2.25 and depends on the assumed relaxivity value.
- This finding is consistent with a pore drying from the centre and the NMR signal originating from fast spin exchange. Alternatively, this can be explained with a continuum of pore sizes and pore throats roughly proportional to each other. This leads to a gradual decrease in T_2 as the applied capillary pressure increases.
- The existence of pores with the same throat size but different body size makes the conclusions valid only on average.

REFERENCES

[1] K. R. Brownstein and C. E. Tarr, "Importance of classical diffusion in NMR studies of water in biological cells," *Phys. Rev. A*, vol. 19, no. 6, p. 2446, 1979.

[2] M. D. Hürlimann, L. L. Latour, and C. H. Sotak, "Diffusion measurement in sandstone core: NMR determination of surface-to-volume ratio and surface relaxivity," *Magn. Reson. Imaging*, vol. 12, no. 2, pp. 325–327, 1994.

[3] M. Fleury, Y. Santerre, and B. Vincent, "Carbonate Rock Typing From NMR Relaxation Measurements," in *SPWLA 48th Annual Logging Symposium*, 2007.